Magnetic relaxation in (Bi, Pb)-2223 superconducting ceramics doped with α-Al_2O_3 nanoparticles

M. Hernández-Wolpez and L. C. Gutiérrez-Rivero
Departamento de Física Universidad de Camagüey,
Ctra. Circunvalación Norte, Km 5 1/2, Camagüey, Cuba.
e-mail: manuel.hwolpes@reduc.edu.cu

I. García-Fornaris
Departamento de Ciencias Básicas Universidad de Granma,
Apartado. 21, Box 85100, Bayamo, Cuba

E. Govea-Alcaide
Departamento de Física, Universidade Federal do Amazonas,
Av. General Rodrigo Octávio, 6200 Coroado I, 69077-000 Manaus, Brazil.

F. Abud, and R. F. Jardim
Instituto de Física, Universidade de São Paulo,
66318, 05314-970, São Paulo, SP, Brasil

P. Muné
Departamento de Física, Universidad de Oriente,
Patricio Lummumba s/n, P. O. Box 90500, Santiago de Cuba, Cuba.

Received 3 July 2019; accepted 9 August 2019

A preliminary study of the magnetic relaxation in (Bi, Pb)-2223 superconducting ceramics doped with α-Al_2O_3 nanoparticles is presented, taking as starting point the measurements of the $M(t)$ dependence, both in samples in the form of powder as in pellet. The relaxation of the three types of vortices that can exist inside these materials is analyzed, emphasizing on the intragranular region where the planar defects exist and, consequently, Abrikosov-Josephson vortices emerge. Finally, interesting results of the comparison between the behavior of the samples in the form of powder and in the form of pellet are shown from the estimation of the pinning energy of the vortices.

Keywords: Bi-based cuprates; magnetic relaxation; vortices; doping; planar defects.

PACS: 74.72.Hs; 74.25.Ha; 74.25.Qt; 74.62.Dh

DOI: https://doi.org/10.31349/RevMexFis.66.42

1. Introduction

Among the type II superconductors, (Bi, Pb)-2223 superconductors ceramics is one of them, these superconducting materials are those in which the magnetic field, when it exceeds the value of the first critical field of the material, penetrates inside of them in form of magnetic flux tubes known as vortices. In the specialized literature, three types of vortices are reported within type II superconductors [1]: Abrikosov's (A), Josephson's (J) and Abrikosov-Josephson's (AJ) vortices [2]. Such vortices emerge in different regions of the material that, in a proper approximation, coincide with the three levels of superconductivity that exist inside these materials: Josephson junctions, cluster or planar defects and crystallites or regions free of defects [3]. It is, therefore, interesting to study how the magnetic flux that penetrates different regions of superconducting ceramics relaxes over time. In that direction one of the most important works, since it is a revision regarding magnetic relaxation in superconductors of high critical temperature, was published by Y. Yeshurun and collaborators [4]. In it, the authors explained the basic concepts for understanding the mechanism studied. They presented several experiments carried out and discussed the main results. Finally, they presented the theoretical models most commonly used to describe it. However, this study of magnetic relaxation in the high critical temperature (**HTc**) superconductors was not related to the three levels of superconductivity, neither to the vortices that emerge in each of them. Magnetic relaxation is typically observed in magnetic dipolar moment measurements in **HTc** using the Vibrating Sample Magnetometer (VSM), or magnetometers based on a Superconducting Quantum Interference Device (SQUID). The magnitude of the dipole moment decreases over time to approximately a logarithmic dependence [4]. A model explaining these effects was proposed and developed by P. W. Anderson [5] and Y. B. Kim [6]. They introduced the basic concept of thermal activation of magnetic flux lines outside the pinning centers which follow a ratio proportional to $\exp(-U/kT)$, where U represents the activation energy, k is the Boltzmann constant, and T is the absolute temperature. This process leads to a redistribution of the magnetic flux lines (vortices) and the current loops associated with them, thus causing a change in the magnetic moment of the superconducting sample over time. The Anderson-Kim model [5, 6] predicted a logarithmic de-

pendence of the magnetic moment with time, as observed by Y. B. Kim and colleagues [7]. According to the conventional Arrhenius relationship, the jump's time is given in terms of the height of the potential energy barrier U, the Boltzmann constant k, and the temperature T as follows:

$$t = t_0 \exp(U/kT). \quad (1)$$

The pre-exponent t_0 (referred to the effective jump attempt time) may differ from the microscopic attempt time by orders of magnitude. The jumping process is assisted by the motive force $\vec{F} = (1/c)\vec{J} \times \vec{B}$. Thus, U must be a decreasing function of J. In the first approximation, the network of barriers is linearly reduced with J in accordance with:

$$U = U_0 \left[1 - J/J_{c0}\right], \quad (2)$$

where U_0 is the height of the barrier in the absence of the conduction force and J_{c0} corresponds to the critical current density in the absence of thermal activation.

This paper presents a study of magnetic relaxation in (Bi, Pb)-2223 superconducting ceramics doped with α-Al_2O_3 nanoparticles, taking as a starting point the measurements of dependence $M(t)$, both in powder and pellet form. The relaxation of the three types of vortices that may exist inside these materials is analyzed, with emphasis on the intragranular region where planar defects exist and consequently the vortices Abrikosov-Josephson emerge. Finally, interesting results are shown from the comparison between the behaviour of the samples in both forms: powder and pellet, from the estimation of the pinning energy of the vortices.

2. Experimental

The samples under study, that have a nominal composition $Bi_{1.65}Pb_{0.35}Sr_2Ca_2Cu_3O_{10+\sigma}$, were obtained using the solid state reaction method [8–12]. The obtained pellets and the α-Al_2O_3 nanoparticles with weight percent in the range 0.1 to 0.7 were milled again in presence of an iso-propyl alcohol solution to avoid agglomeration [13]. The alcohol was evaporated as the mixture was shaken. Finally, the powders were again ground and compacted at a uniaxial pressure of 249 MPa to obtain cylindrical samples with dimensions of: $d = 10$ mm diameter and $h = 1$ mm thickness. The last heat treatment was done, in all cases, in air at $845°$C for 12 h followed by slow cooling. In the discussion presented in this paper, samples were prepared in pellet form as well as in powder form, from the ceramics obtained, according to Table I.

TABLE I. Percentage in weight of nanoparticles of α-Al_2O_3, temperature of the superconducting transition of the samples.

Code	% wt of α-Al_2O_3	$T_{\text{coff}}(K)$
B00	0.0	95.5
B03	0.3	101.9
B05	0.5	98.3

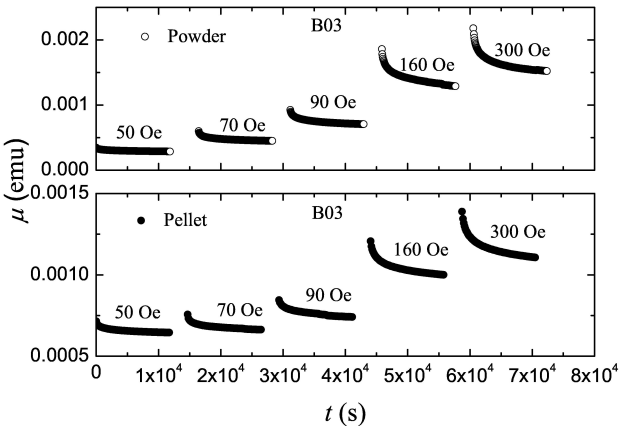

FIGURE 1. Magnetic moment as a function of time corresponding to a powder sample and pellet sample of the ceramic B03.

To obtain the relaxation curves of the magnetization ($M(t)$) a sequence was used in the SQUID as follows. The sample was cooled in zero field cooling (ZFC) to 77 K. After stabilization, a determined value of the magnetic field intensity was applied, H_{am} = 50 Oe, during a short time of the order of 40 s, and the field was removed at the same time that the magnetic moment was measured during a long time of the order of 12 000 s. In the like manner, the sequence continued for different H_{am} values (70, 90, 120, 160, and 300 Oe). However, before each new value was set, the temperature of the sample was increased above the critical temperature (T_c) to clear the "magnetic history". The magnetic moments were obtained from the experiment. Then, the magnetic moments were divided by the masses of the samples to obtain the corresponding magnetizations, and thus to see the differences that cause the different values of H_{am} in the relaxation of each sample. These procedures were done in powder and pellet samples. When comparing the results between several samples (in powder or pellet form or different amounts of α-Al_2O_3 nanoparticles) the magnitude to be compared should be normalized. A preliminary interpretation of the behaviour of magnetic relaxation in powder and pellet samples allows two important features to be extracted (see Fig. 1): a) as the value of the maximum applied magnetic field intensity increases, the relaxation mechanism is significantly noticeable and b) if the measured curves are compared to the same values of maximum applied magnetic field intensity, this mechanism is always more notable in the case of the powder sample.

3. Results and discussion

From the measurements of the dependence, ($M(t)$), both in powder and pellet forms (see Fig. 1), the relaxation of the three types of vortices present inside these materials are analyzed. Outstanding results of the comparison between the behaviour of the samples in powder

TABLE II. Decay rates of normalized magnetization in ceramics B00, B03 and B05 in powder and pellet form.

Samples	H_{am} (Oe)	$\Delta M/Mn$max(%)
	300	35.7
B00 Powder	90	21.6
	70	17.5
	300	30.1
B03 Powder	90	23.5
	70	25.1
	300	23.7
B05 Powder	90	19.5
	70	18.8
	300	30.3
B00 Pellet	90	23.2
	70	22.8
	300	22.6
B03 Pellet	90	13.6
	70	12.3
	300	16.6
B05 Pellet	90	8.7
	70	8.2

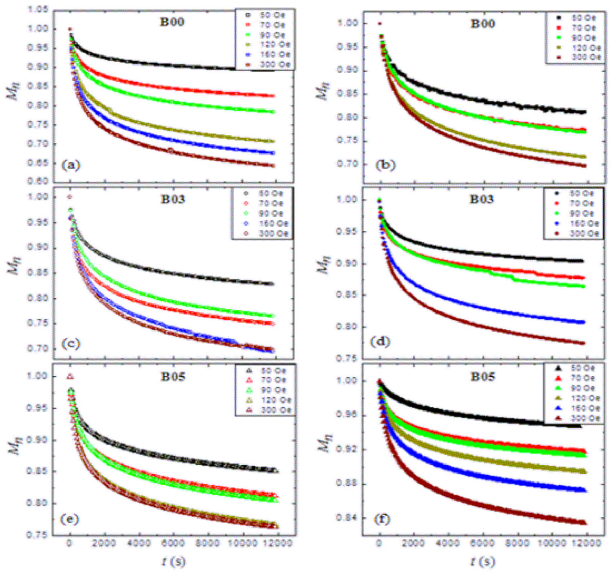

FIGURE 2. Dependence of the remanent magnetization as a function of time, ($Mn(t)$), corresponding to the ceramics B00 (powder: (a) and pellet: (b)), B03 (powder: (c) and pellet: (d)) and, B05 (powder: (e) and pellet: (f)).

and pellet forms are also shown. Throughout the entire paper, the study will be conducted, emphasizing on the intragranular region, where planar defects [14–17] exist and, therefore, AJ vortices emerge [2].

The Fig. 2 shows relaxation curves of the normalized magnetization corresponding to the three ceramics B00, B03 and B05. These curves were obtained from data similar to those shown in Fig. 1, which are those obtained directly from the experiment. All measurements were made at the 77 K.

Table II lists the values of the decay rate of the normalized remanent magnetization obtained using Eq. (3). The comparison between these values allows a quantitative analysis of the behavior of the samples. This analysis can help in the understanding of the relaxation mechanism of the AJ vortices and to correlate this behaviour with other measured samples of the same ceramics.

$$\Delta Mn/Mn_{\max} \tag{3}$$

where, $\Delta Mn = Mn_{\max} - Mn(12000s)$. This calculation makes it possible to determine in a better and more precise manner the differences in the behaviour of the samples measured for each of the values of the maximum intensity of the magnetic field applied to the measurements appearing in the Table II. If you look at the same table in detail, you can see that samples B03 and B05 in pellet form have the lower drop rate values of the normalized magnetization. This result leads to the fact that they have the best trapping properties, which does not correspond to what was published earlier [13] in the case of the B05 sample. Due to this lack of correspondence between several results, the determination of the pinning energy is presented from the relaxation measurements of the remaining magnetization. Among the works that have studied the relaxation of magnetization in the **HTc**, P. Chaddah and K. V. Bhagwat determined the pinning potential using the following equation [18]:

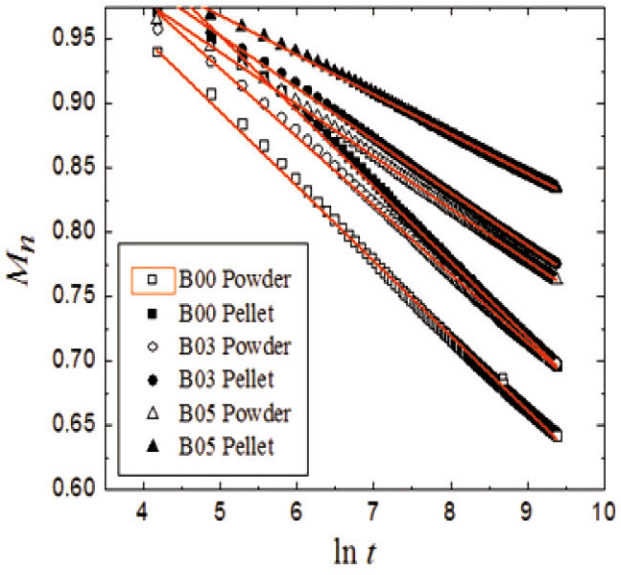

FIGURE 3. Dependence of the remanent magnetization Mn as a function of the logarithm of time $\ln t$ corresponding to all samples measured at a maximum applied magnetic field intensity of 300 Oe with their respective fitting.

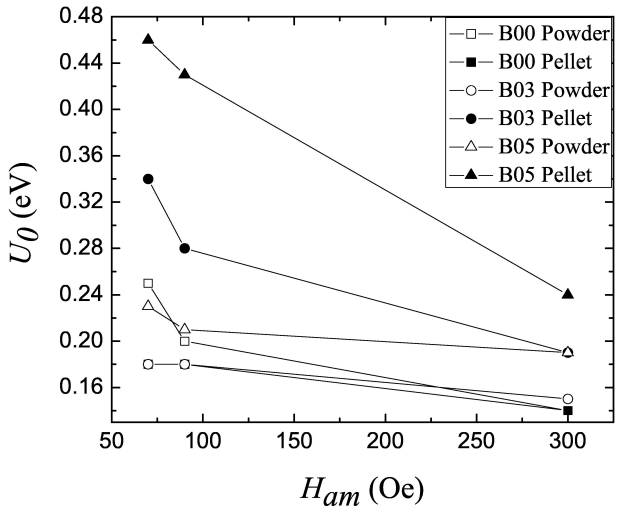

FIGURE 4. Effective pinning energy as a function of applied magnetic field for all samples.

$$Mn(t) = Mn_0\,[1 - (kT/U_0)]\ln t \qquad (4)$$

where Mn is the normalized magnetization, Mn_0 is the initial normalized magnetization, k is the Boltzmann constant, T is the temperature at which the measurement is made which, in this case, was 77 K and U_0 is the potential pinning energy.

The Fig. 3 shows how to obtain the U_0 values from the relaxation measurements of the normalized magnetization. The linear fittings applied to each of the curves from which, following Eq. (4), the values of U_0 are determined for each of the samples and with an applied magnetic field strength value of 300 Oe. Table III contains the determined U_0.

From Table III it can be noticed the confirmation of the result interpreted from Table II and it is the fact that from this analysis the sample B05 in pellet form has the highest pinning energy for 300 Oe, value of the intensity of the applied magnetic field where it is supposed that the crystals have been totally penetrated. It could be thought that the lack of correspondence between the pinning energies measured for the samples by the electric transport route [19] and by the magnetization relaxation route presented in this paper (see Table III) reveal that the two results are counterposed. The cause of this interesting physical fact is explained below.

TABLE III. Pinning energy values for a maximum applied magnetic field intensity of 300 Oe corresponding to all the samples studied under this heading.

Samples	$U_{0(300\text{Oe})}$ (eV)
B00 Powder	0.14
B00 Pellet	0.14
B03 Powder	0.15
B03 Pellet	0.19
B05 Powder	0.19
B05 Pellet	0.24

For transport measurements it is sample B03 it is the one with the best properties because it has the highest pinning energy values [19], while for the magnetic relaxation, sample B05 in pellet form that has the highest pinning energy value. In the case of the latter, the result provides information of the pinning in the whole sample, but having been totally penetrated the crystallites, so that the three types of vortices contribute to the result and, as in this case, no current is applied to the sample, all the vortices that penetrated and were trapped in each of the regions (or different levels of superconductivity) remain either by the effects of the presence of intragranular planar defects [14–17] or by the presence of α-Al_2O_3 nanoparticles (pores). Such an effect that is revealed in the behavior of the B05 sample in pellet form, is impossible to detect from transport measurements, for only taking into account that a current is applied to the sample the conditions are modified and the effects of that modification influence especially in the J that have the lower energies and by the action of the Lorentz force are expelled from the material even without being able to be detected for values of intensity of the applied magnetic field less than 300 Oe [19].

Finally, in Fig. 4 all the values of pinning energy for each one of the samples in powder and pellet form corresponding to the three values of intensity of the applied magnetic field (70, 90, 300) Oe are shown. The difference between pinning energy values for 70 Oe is greater than 300 Oe ($\Delta_{70\text{Oe}} > \Delta_{300\text{Oe}}$), it that in the case of magnetic relaxation, as static measurement and all types of vortices are involved (when the crystallites have been totally penetrated) while for 70 Oe only Josephson's vortices are involved.

4. Conclusions

The B05 sample in pellet form has the lowest drop rate values of the normalized magnetization (see Table II) and in turn the highest value of U_0 for 300 Oe of maximum applied magnetic field intensity. Which represent the best pinning energy of the magnetic flux from this measurements. Consequently, the resulting remanent magnetization, which includes, in general, the three types of vortices, relaxes more slowly when there is no transport current applied to this sample, while by means of voltage relaxation the sample B03 presents the best pinning properties of the magnetic flux. The relaxation dependencies of magnetization $M(t)$, and voltage $V(t)$, are not equivalent. Thus, for the first the sample B05 in pellet form has a better pinning of the magnetic flux and for the second it is B03 that presents it. On the other hand, the fact $\Delta_{70\text{Oe}} > \Delta_{300\text{Oe}}$ (0.28 eV $>$ 0.10 eV) allows to correlate this behavior with the different percent in weight of α-Al_2O_3 nanoparticles and the three types of vortices that exists inside of this materials, because the effect of the presence of nanoparticles is more remarkable for 70 Oe than 300 Oe, due to in the second case the samples have already been totally penetrated.

Acknowledgments

This work was supported by the Fundação Coordenação de Aperfeiçoamento de Pessoal de Nível Superior (CAPES) under Grant No. 104/10. R.F.J. acknowledges support from Brazil's agencies FAPESP (Grants No. 2013/07296-2, and No. 2014/19245-6) and CNPq (Grants No. 444712/2014-3 and No. 306006/2015-4.

1. A. Gurevich, *Phys. Rev. B* **48** (1993) 12857-12865.
2. A. Gurevich, and L. D. Cooley, *Phys. Rev. B* **50** (1994) 13563-13577.
3. M. Hernández-Wolpez, A. Cruz-García, R. F. Jardim, and P. Muné, *J. Mater. Sci.: Mater. Electron*. **28** (2017) 15246-15251.
4. Y. Yeshurun, A. P. Malozemoff, and A. Shaulov, *Rev. Mod. Phys*. **68** (1996) 911-949.
5. P. W. Anderson, *Phys. Rev. Lett*. **9** (1962) 309-311.
6. P. W. Anderson, and Y. B. Kim, *Rev. Mod. Phys*. **36** (1964) 39-43.
7. Y. B. Kim, C. F. Hempstead, and A. R. Strand, *Phys. Rev. Lett*. **9** (1962) 306-309.
8. P. Muné, E. Govea-Alcaide, and R. F. Jardim, *Physica C* **384** (2003) 491-500.
9. E. Govea-Alcaide, PhD Thesis, University of Havana, 2005.
10. I. García-Fornaris, E. Govea-Alcaide, M. Alberteris-Campos, P. Muné, and R. F. Jardim, *Physica C* **470** (2010) 611-616.
11. E. Govea-Alcaide, I. García-Fornaris, P. Muné, and R. F. Jardim, *Eur. Phys. J. B*. **58** (2007) 373-378.
12. E. Govea-Alcaide, P. Muné, I. García-Fornaris, and R. F. Jardim, *In: YBCO Superconductor Research Progress*. edited by L-C. Liáng, (Nova Science Publishers, Inc 2007), pp. 1-27.
13. M. Hernández-Wolpez, I. García-Fornaris, E. Govea-Alcaide, R. F. Jardim, and P. Muné, *Rev. Mex. Fis*. **64** (2018) 127-131.
14. V. Kataev, N. Knauf, B. Büchner, and D. Wohlleben, *Physica C* **184** (1991) 165-171.
15. O. Eibl, *Physica C* **168** (1990) 249-256.
16. K. Kishida, and N. D. Browning, *Physica C* **351** (2001) 281-294.
17. M. Hernández-Wolpez, E. Martínez-Guerra, R. F. Jardim, and P. Muné, *Rev. Mex. Fis*. **62** (2016) 515-525.
18. P. Chaddah and K. V. Bhagwat, *Phys. Rev. B* **43** (1991) 6239-6241.
19. M. Hernández-Wolpez *et al., J. Mater. Sci.: Mater. Electron*. **29** (2018) 5926-5933.